Copy 46

DECLASSIFIED

CONFIDENTIAL

NASA TM SX-848

NASA TM SX-848

IN-02
380476
34P

GROUP 3
Downgraded at 12-year
intervals; not automatically
declassified

TECHNICAL MEMORANDUM

SX-848

Declassified by authority of NASA
Classification Change Notices No. 212
Dated ** 31 MAR 1971

CLASSIFICATION CHANGED
TO UNCLASSIFIED
By Authority of T.O. 71-75 Date 1-12-71

for the

Bureau of Weapons, Department of the Navy

FULL-SCALE WIND-TUNNEL INVESTIGATION OF THE DRAG CHARACTERISTICS OF AN HU2K HELICOPTER FUSELAGE

TED NO. N-AM-110

By William I. Scallion

Langley Research Center
Langley Station, Hampton, Va.

CASE FILE COPY

CLASSIFIED DOCUMENT - TITLE UNCLASSIFIED

This material contains information affecting the national defense of the United States within the meaning of the espionage laws, Title 18, U.S.C., Secs. 793 and 794, the transmission or revelation of which in any manner to an unauthorized person is prohibited by law.

NATIONAL AERONAUTICS AND SPACE ADMINISTRATION
WASHINGTON

JUN 27 1963

CONFIDENTIAL

NATIONAL AERONAUTICS AND SPACE ADMINISTRATION

TECHNICAL MEMORANDUM SX-848

for the

Bureau of Weapons, Department of the Navy

FULL-SCALE WIND-TUNNEL INVESTIGATION OF THE DRAG CHARACTERISTICS OF AN HU2K HELICOPTER FUSELAGE*

TED NO. N-AM-110

By William I. Scallion

SUMMARY

An investigation was conducted in the Langley full-scale tunnel to determine the drag characteristics of the HU2K helicopter fuselage. The effects of body shape, engine operation, appendages, and leakage on the model drag were determined.

The results of the tests showed that the largest single contribution to the parasite drag was that of the rotor hub installation which produced about 80 percent of the drag of the sealed and faired production body. Fairings on the rotor hub and blade retentions, or a cleaned-up hub and retentions, appeared to be the most effective single modifications tested. The total drag of all protuberances and air leakage also contributed a major part of the drag - an 83-percent increase over the drag of the sealed and faired production body. An additional increment of drag was caused by the basic shape of the fuselage - 19 percent more than the drag obtained when the fuselage shape was extensively refaired. Another sizable increment of drag was caused by the engine oil-cooler exit which gave a drag of 8 percent of that of the sealed and faired production body.

INTRODUCTION

At the request of the Bureau of Weapons, U.S. Navy, an investigation of the drag characteristics of the HU2K helicopter fuselage was conducted in the Langley full-scale tunnel. The purpose of this investigation was to determine the effect of body shape, engine operation, appendages, and leakage on the drag of the helicopter body. The incremental drag contribution of each change in body shape, each major appendage, the cooling system, and the rotor hub and blade retentions was determined. The data are presented without detailed analysis, but, some of the more pertinent factors observed are pointed out and discussed.

---

*Title, Unclassified.

SYMBOLS

The data presented herein are referred to the wind system of axes. The positive directions of forces, moments, and angular displacements are shown in figure 1.

F_D	drag, lb
F_L	lift, lb
i_t	horizontal-tail incidence (relative to fuselage reference line), deg
$M_{Y,w}$	pitching moment, ft-lb
q	dynamic pressure, lb/sq ft
α	angle of attack of fuselage reference line, deg
Δ	incremental force or moment

MODEL

The model was a production HU2K fuselage equipped with the rotor hub, blade retentions, stub blades, blade cuffs, tail rotor, tail landing gear, auxiliary tanks, cargo hook, horizontal tail, and radio antennas. The engine and power accessories were installed. Sketches of the model are shown in figures 2 and 3 and photographs of the model and modifications are shown in figure 4. Fuselage modifications furnished by the manufacturer consisted of a large fuselage afterbody fairing, a modified nose section or windshield, cabin roof fairing, and front and rear sponson fairings (see fig. 3). In addition to these modifications, a large fillet was installed at the juncture of the top of the sponsons, and the rear tiedown rings were faired over. These modifications and their locations can be seen in figures 3, 4(a), and 4(b). All openings were sealed with tape and small protuberances were faired over. For tests with the body sealed and faired, the engine inlet was faired over and sealed, the tailpipe was removed, and the opening was faired and sealed. For power-on tests of the basic faired body (with all shape modifications installed, faired, and sealed) a flush tailpipe was fabricated and installed. The effective thrust angle of this tailpipe was 63.4° to the plane of symmetry as compared with 11.8° for the production tailpipe.

TESTS

The tests were conducted for an angle-of-attack range of -8.5° to 3.5°. The average tunnel velocity was 156 fps corresponding to a dynamic pressure of 29 lb/sq ft. The general test plan consisted of first testing the model with all appendages removed, all modified shape fairings installed, the engine inlet and tailpipe faired and sealed over, and all openings and protuberances sealed and faired. During the tests, the modifications were progressively removed until the sealed and faired production shape was reached. The appendages were then progressively installed and seals were removed until the production configuration was complete. By this method, the incremental drag of the various components was determined.

Several tests were conducted with the engine operating to simulate the engine inlet and tailpipe gas-flow effects on the drag of the body. It was desirable to operate the engine at high power in order to simulate properly the gas flows, but, this was not possible. The power-on tests without the rotor hub were conducted with the rotor brake locked, but the engine load was limited to the capacity of the rotor brake. This procedure resulted in a gas-generator speed of about 74 percent with the power turbine locked at 0 percent. The engine power was quite low for these conditions, and the residual thrust was not attainable from the available manufacturer's data. For this reason, the power-on drag data include the residual engine thrust values.

The power-on tests with the rotor hub installed were conducted at 100-percent rotor speed resulting in a gas-generator speed of 74 percent.

CORRECTIONS AND ACCURACIES

The angle-of-attack data were corrected for a tunnel stream misalinement of -0.5°, and the drag data were corrected for tunnel buoyancy effects and model-support-strut drag tares.

The following accuracies were estimated to exist during the tests:

F_D, lb	±0.3
F_L, lb	±2.0
$M_{Y,W}$, ft-lb	±6.6
q, lb/sq ft	±0.29

PRESENTATION OF DATA

A description of the model test conditions is given in table I for each run represented in the figures. Table II presents a summary of the incremental drag values for the changes in body shape, appendages, and leakage. These values were obtained by subtracting the total drag of one configuration from that of another, and therefore include the interference effects between the fuselage and the various components.

Figure 5 shows the variation of drag with angle of attack for the body shapes tested. The effects of appendages and leakage on drag, lift, and pitching moment are shown in figure 6. Figure 7 shows the effect of engine operation and tailpipe configuration on the drag characteristics of the fuselage. The residual thrust of the engine is included in the data. The effects of the original and modified engine oil-cooling systems are shown in figure 8. The effects of the rotor hub, retentions, stub blades, and cuffs on the drag, lift, and pitching moment of the model are presented in figure 9. The drag of the model as affected by a plywood ramp installed on the nacelle with the hub and retentions rotating is shown in figure 10. Figure 11 presents the effect of tail-rotor installation on the model drag characteristics with the rotor adjusted to a nonlifting condition. The local-to-free-stream dynamic-pressure ratios in the region of the rotor hub and retentions are shown in figure 12.

DISCUSSION

Effect of Body Shape

As shown in figure 5, the minimum equivalent parasite area obtained from tests of the basic refaired body was 3.80 square feet. An estimation of the parasite area based on wetted area resulted in a value of 3.00 square feet. The difference in these two values is indicative of the drag rise due to the variation in body shape and surface conditions from that of a streamlined body with the same wetted area. At an angle of attack of -6.5° (approximately the angle for cruise) the parasite area of the production body shape was 5.03 compared with 4.21 for the basic refaired body shape. This amounted to a 19-percent increase in parasite drag. The most effective modifications in shape, as shown by figure 5 and table II, were the cabin roof fairing, tail rotor pylon fairing, and sponson afterbody fairing.

Effect of Protuberances

In general, no major factor was found to contribute significantly to the overall drag of the model, but the total parasite drag of the production body shape was increased 83.5 percent by appendages, protrusions, and leakage. References 1 and 2 have also shown that where the body shape was relatively clean, the drag was increased appreciably by leakage and improper fairing of small protrusions. The total drag increment caused by leakage and small protrusions such as windshield posts, tiedown rings, and exposed hinges was about 0.85 square foot. This increment amounted to 22 percent of the total equivalent parasite area of the basic refaired body, or 9 percent of that of the production body in the service condition. Part of the increment in parasite area included that caused by handhold doors on the front of the engine nacelle that blew in during the tests.

Effects of Engine Power and Cooling System

The effects of engine-exhaust flow on drag for two tailpipe installations are presented in figure 7. Although neither of the tailpipe installations is considered good from a drag standpoint, the results do indicate two sources for possible drag improvement. A comparison of the power effects on the model with the faired afterbody and flush tailpipe and on the model with the production nacelle and tailpipe shows that the overall drag was less for the former configuration despite the fact that the thrust from this tailpipe was oriented so that it contributed about only one-half as much to drag reduction as did the original tailpipe. (Note that the engine residual thrust is included in the data in fig. 7.) As noted earlier, the power output of the engine was low for these tests, and it cannot be assumed that the power-on results would be the same for higher engine-power output and residual thrust. However, these results do indicate that minimizing the frontal area of the exhaust system, if combined with an effective thrust angle near zero, would produce the maximum drag reduction.

As shown in figure 8(a), the original cooling system, when operating, increased the equivalent parasite area of the model in forward flight. As a concession to the hovering cooling requirements, the cooling system used an engine-driven fan which forced cooling air through the oil cooler and exhausted directly from the top of the nacelle. This cooling exit may be seen in figures 2(a) and 4(d). The cooling air exhausting in this manner contributed nothing to thrust and caused separation on the aft portion of the engine nacelle, and consequently caused an increase in the parasite drag of 8 percent over that of the sealed and faired production body. As shown in figure 8(b), installation of a louvered cooling exit resulted in a decrease in the parasite drag approximately equal to the increase caused by the original system.

Effect of Rotor Hub Configuration

As shown in figure 9(a), installation of the rotor hub and retentions greatly increased the parasite drag by about 80 percent over that of the sealed and faired production body. The data indicate, however, that cleaning up the hub and retentions or installation of the cuffs produced sizable reductions in drag. The two configurations are not directly comparable with each other, because the cleaned-up hub and retentions did not have the blade stubs installed. An approximate comparison between the cuffs and the cleaned-up hubs and retentions, however, may be seen by comparing the dashed curve in figure 9(a) with the drag curve for the cuffs. This comparison shows that the cuff configuration produced less drag than that of the cleaned-up retentions at angles of attack below -6.5°; however, at $\alpha = -6.5^{\circ}$ and above, the drag of the cuffs was greater than the cleaned-up configuration. It can be noted in figure 9(b) that the blade stubs and cuffs produced a negative lift increment, and therefore, the drag associated with these components includes some induced drag in addition to parasite drag. The angle of attack of the blade and cuff was fixed by the angle at which the rotor pitch locks restrained the blade from angular motions, and this angle could not be adjusted.

Part of the rotor hub drag was attributable to an increase in local dynamic pressure in the region of the hub caused by the presence of the engine nacelle. This increase in dynamic pressure, as obtained from flow surveys, is shown in figure 12.

The results of a preliminary test with a ramp installed are shown in figure 10. Examination of the data indicated that the ramp produced a small decrease in rotor hub parasite drag, but the ramp installation caused a net increase in drag.

SUMMARY OF RESULTS

The results of tests to determine the drag characteristics of the HU2K fuselage may be summarized as follows:

1. The largest single contribution to parasite drag was that of the rotor hub and blade retentions. Their drag was about 80 percent of that of the sealed and faired production body. This drag increment was reduced by the use of a cleaned-up hub and retentions.

2. The drag increment added by all the fuselage protuberances and air leakage was about the same as that of the rotor hub, but was made up of the small drag increments of many items, no one of which was very large.

3. The drag of the original cooling system, amounting to about 8 percent of the drag of the sealed and faired production body, was eliminated by the addition of a louvered exit.

4. The form drag of the production body shape was about 19 percent higher than that obtained when the fuselage was extensively refaired.

Langley Research Center,
National Aeronautics and Space Administration,
Langley Station, Hampton, Va., June 4, 1963.

REFERENCES

1. Lange, Roy H.: A Summary of Drag Results From Recent Langley Full-Scale-Tunnel Tests of Army and Navy Airplanes. NACA WR L-108, 1945. (Formerly NACA ACR L5A30, 1945.)

2. Jenkins, Julian L., Jr., Winston, Matthew M., and Sweet, George E.: A Wind-Tunnel Investigation of the Longitudinal Aerodynamic Characteristics of Two Full-Scale Helicopter Fuselage Models With Appendages. NASA TN D-1364, 1962.

TABLE I.- DESCRIPTION OF DATA RUNS

Run	Description
1	Basic faired body. Main afterbody fairing, modified windshield and cabin roof fairing, front and rear sponson fairings, fillets at sponson-fuselage juncture, and tail pylon afterbody fairing installed. Engine inlet sealed and tailpipe removed and opening sealed. All external appendages removed. All openings and junctures sealed and faired. Wheel well covered and sealed.
2	Same as run 1 with engine inlet open, aft oil-cooler exit open, and flush tailpipe installed. Engine not operating.
3	Same as run 2. Engine operating with rotor brake on.
4	Main afterbody fairing removed. Production tailpipe installed. Engine not operating.
5	Same as run 4. Engine operating with rotor brake on.
6	Engine inlet sealed, tailpipe removed, and nacelle faired over. Aft cooling exit sealed.
7	Same as run 6 with tail pylon afterbody fairing removed.
8	Same as run 7 with rear sponson fairing removed.
9	Same as run 8 with front sponson fairing removed.
10	Same as run 9 with cabin roof fairing removed.
12	Basic production body. Same as run 10 with production windshield installed.
13	Same as run 12 with tail rotor gearbox, shaft, and spider installed.
14	Same as run 13 with all additional test fairings and fillets removed.
15	Same as run 14 with tail gear installed.
16	Same as run 15 with windshield wipers, temperature sensor, pitot tube, relief tube venturi, cargo hook, bulged windows, IFF, UHF, Loop, TACAN and ARC 59 antennas, and rotating beacon installed. Tail pylon hand hold unsealed.
17	Same as run 16 with engine nacelle and tail rotor shaft tunnel unsealed.
18	Same as run 17 with tail rotor gearbox cooling openings unsealed.

TABLE I.- DESCRIPTION OF DATA RUNS - Concluded

Run	Description
19	Same as run 18 with landing gear sponsons and body underside unsealed.
20	Same as run 19 with cabin, cargo doors, and nose unsealed.
21	Same as run 20 with wheel well covers removed.
22	Wheel well covers reinstalled. Same as run 20 with stabilizer installed at $i_t = 10^\circ$.
23	Same as run 22 with auxiliary tanks installed.
24	Auxiliary tanks removed. Engine inlet open, tailpipe installed, and cooling system sealed. Engine operating with rotor brake installed.
25	Cooling-system evaluation. Same as run 24 with cooling system unsealed. Engine operating.
26	Blade hub, retentions, blade stubs, and cuffs installed. Engine operating.
27	Same as run 26 with blade cuffs removed.
28	Same as run 27 with tail rotor installed and rotating.
29	Same as run 28 with tail rotor removed. Revised cooling exit with louvers installed.
30	Same as run 29 except original cooling exit installed. Stub blades removed. Hub and retentions remain.
31	Same as run 30 with plywood ramp installed.
32	Plywood ramp removed. Cleaned-up hub and retentions. Engine operating.
34	Rotor hub and retentions removed and opening faired over. Engine operating. Plywood ramp installed.

TABLE II.- SUMMARY OF DRAG CHARACTERISTICS OF FUSELAGE

Item	$\Delta F_D/q$, ft^2		F_D/q, ft^2
	$\alpha = -0.5^\circ$	$\alpha = -6.5^\circ$	$\alpha = -6.5^\circ$
Basic faired and sealed body shape			4.212
Afterbody fairing removed	0.140	0.113	
Tail pylon fairing removed	.320	.430	
Rear sponson fairing removed	.253	.022	
Front sponson fairing removed	-.036	-.033	
Cabin roof fairing removed	.309	.112	
Modified windshield removed	.079	.171	
Basic production body shape sealed and faired			5.027
Tail rotor gearbox added	.737	.626	
Additional nonproduction fairings removed	.380	.512	
Tail wheel installed	.443	.404	
Production fairings, tiedown rings, windshield wipers, temperature sensor, bulbous windows, IFF, UHF, Loop, TACAN and ARC 59 antennas, and rotating beacon installed	.414	.421	
Engine nacelle and tail rotor tunnel unsealed	.121	.161	
Tail rotor cooling system unsealed	.362	.439	
Sponsons unsealed	.072	.099	
Cabin and nose unsealed	.113	.074	
Wheel well doors removed	.357	.341	
Stabilizer installed, $i_t = 10^\circ$	1.024	1.120	
Production body unsealed with appendages installed			9.224

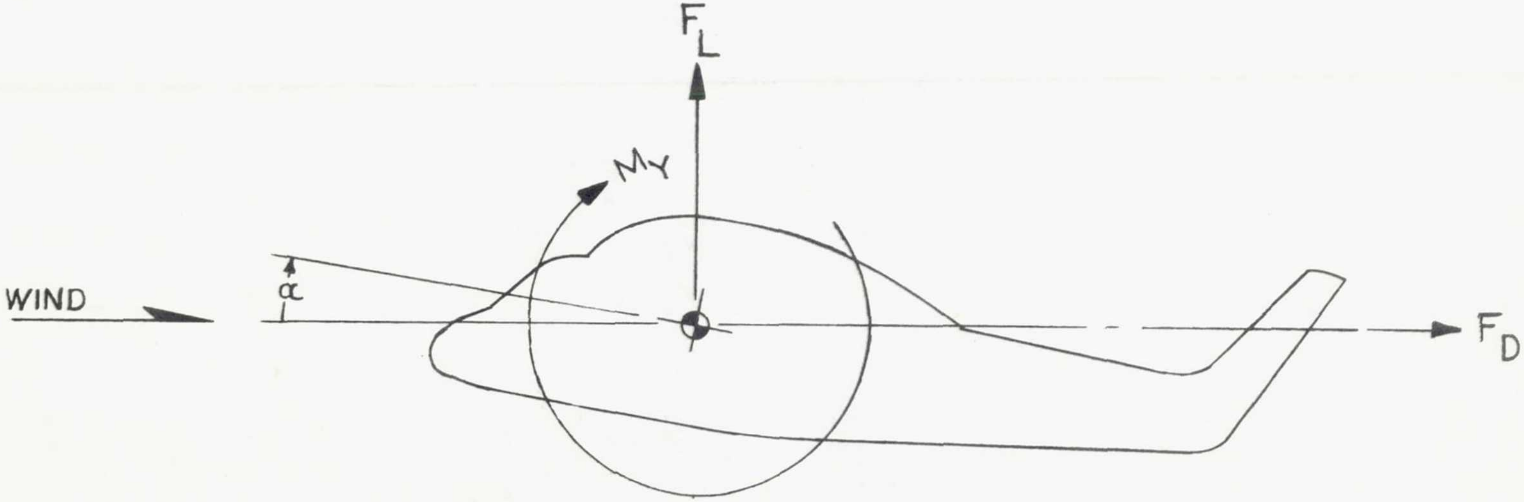

Figure 1.- Axis systems used. Positive directions of forces and moments shown.

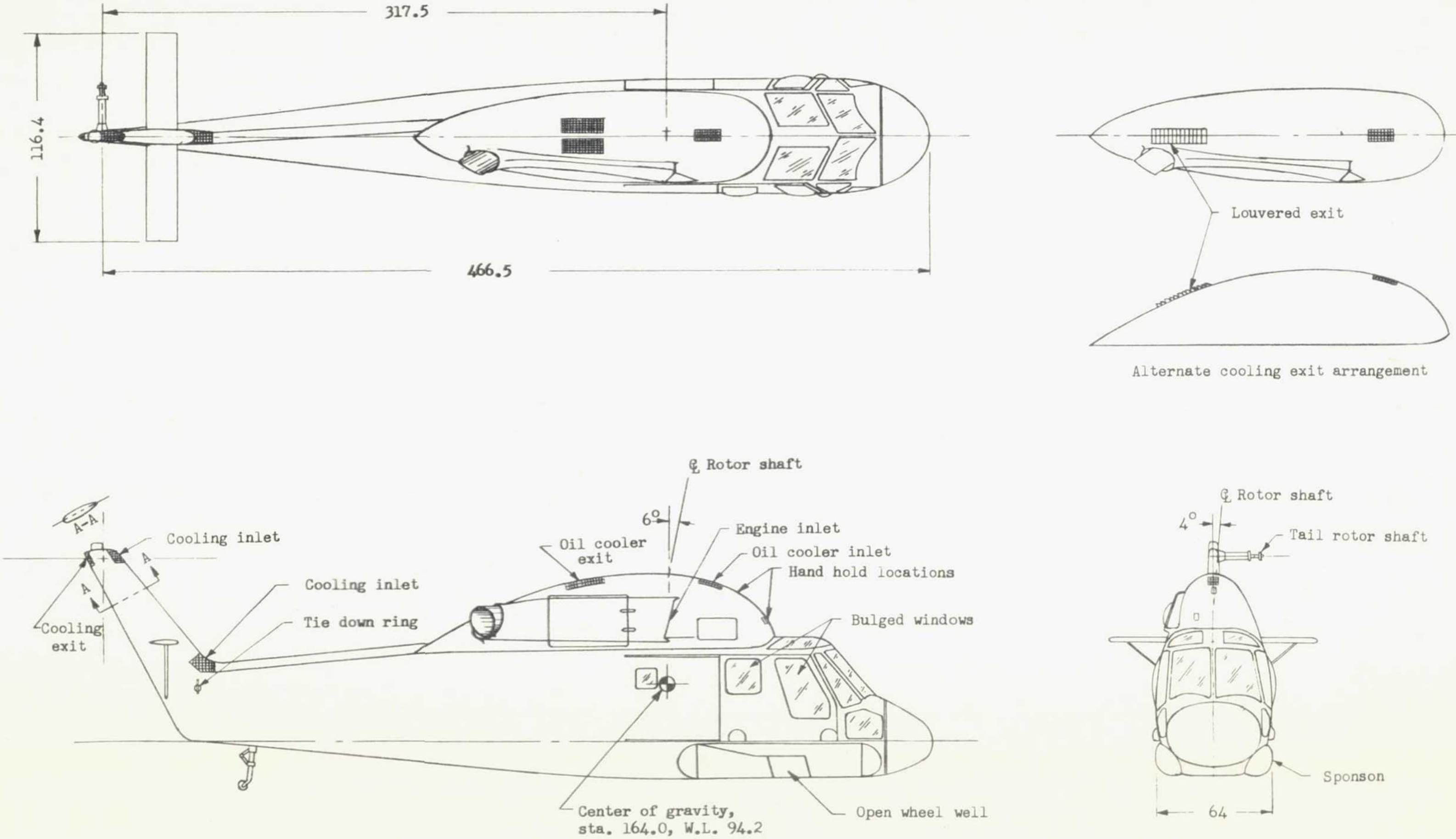

(a) Three-view sketch of production fuselage.

Figure 2.- Sketches of model. All dimensions are in inches.

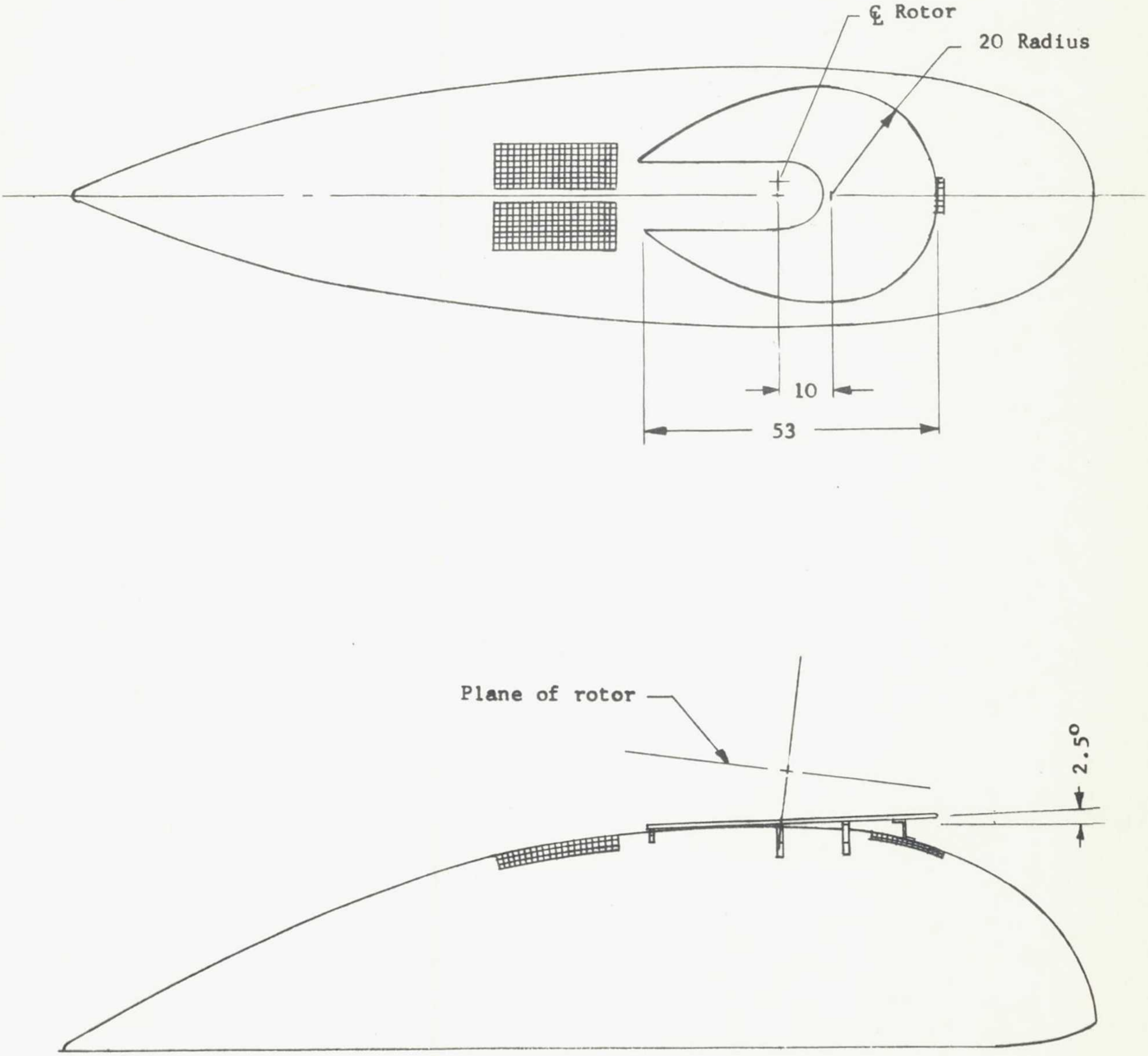

(b) Details of plywood ramp installed on nacelle.

Figure 2.- Concluded.

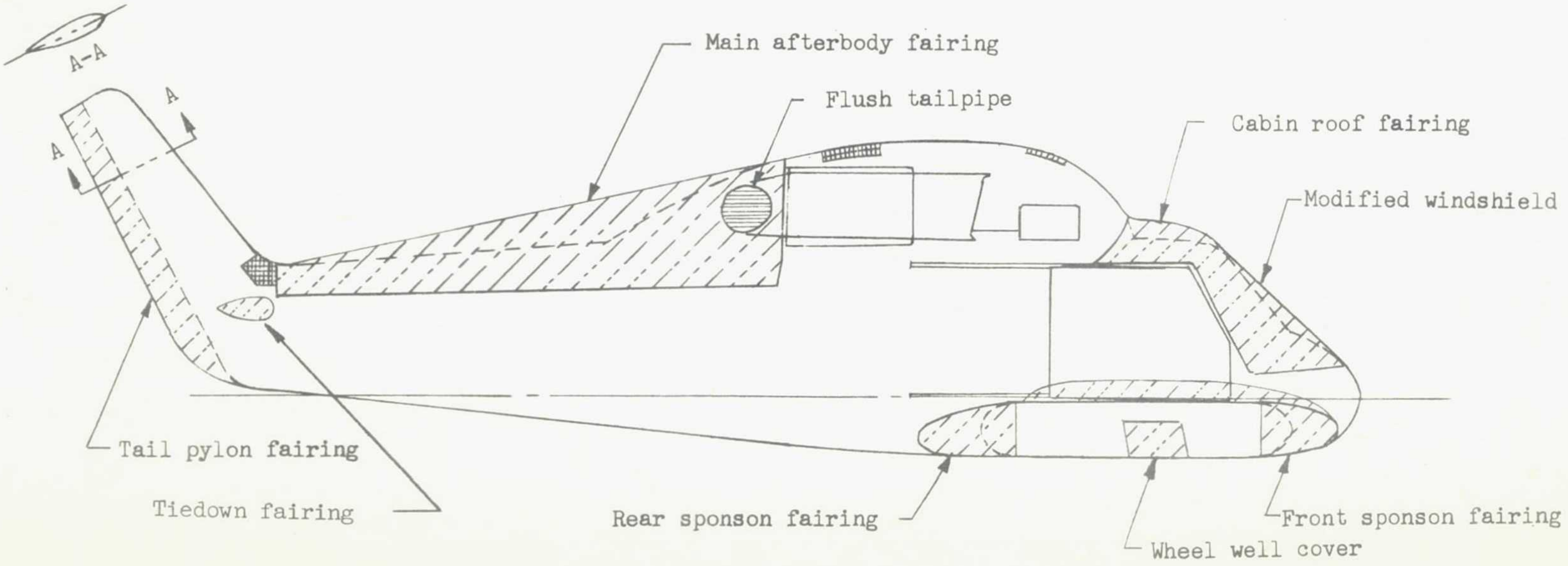

Figure 3.- Sketch of basic faired body, showing all major fairings.

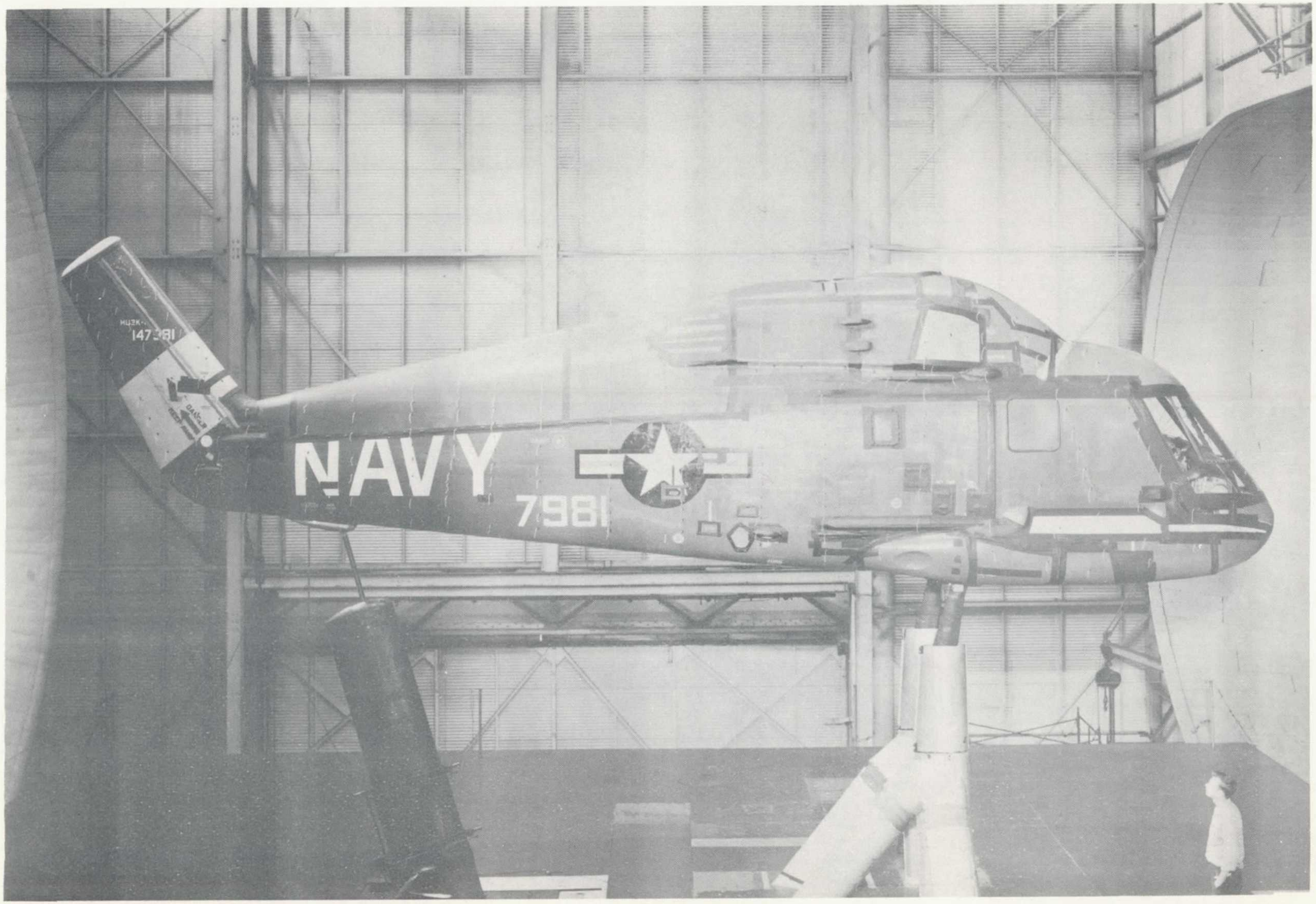

(a) Basic faired body. L-61-4692

Figure 4.- Photographs of HU2K fuselage and modifications.

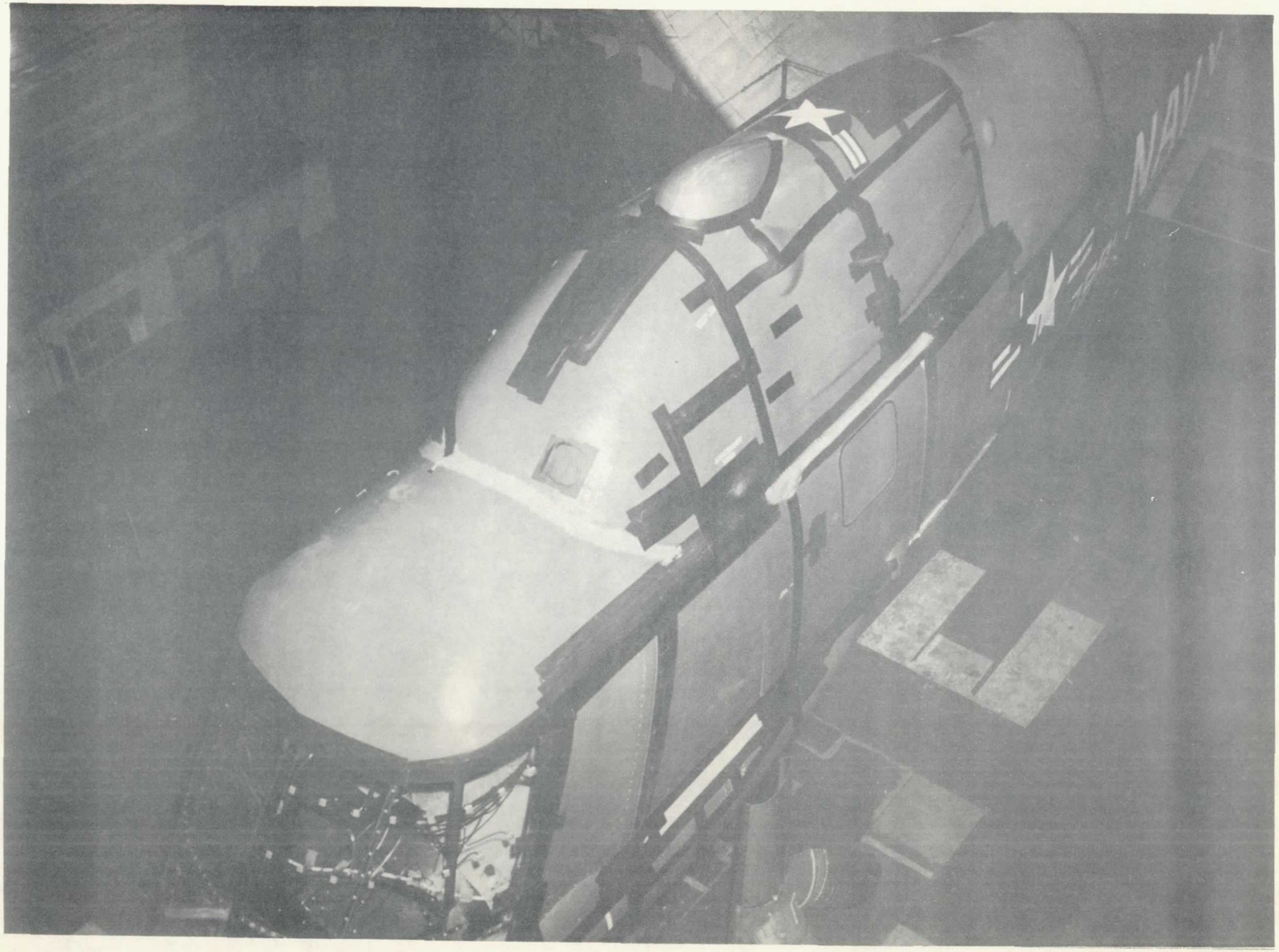

(b) View of basic faired body, showing cabin roof fairing.

L-61-4697

Figure 4.- Continued.

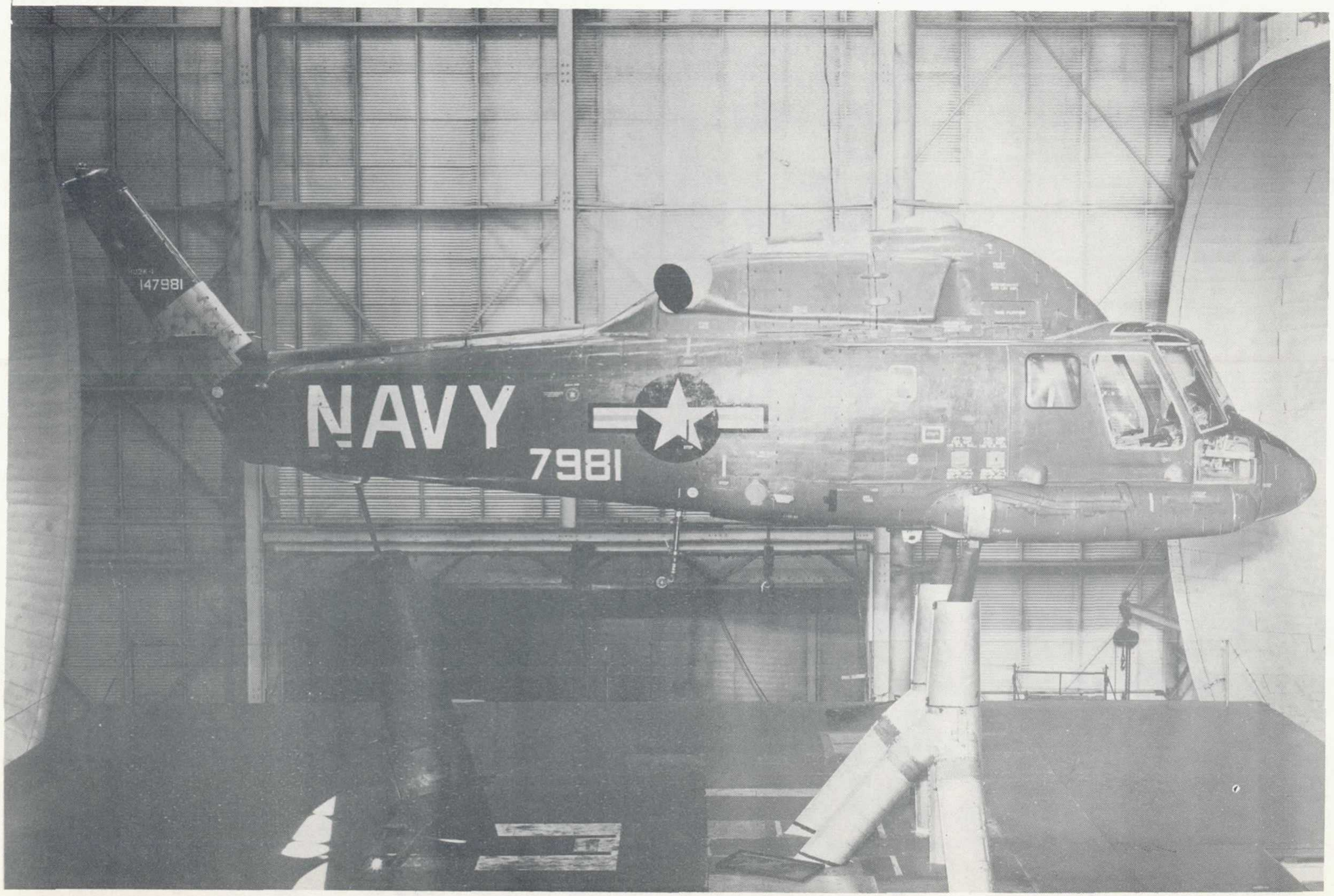

(c) Basic production body with appendages. L-61-6057

Figure 4.- Continued.

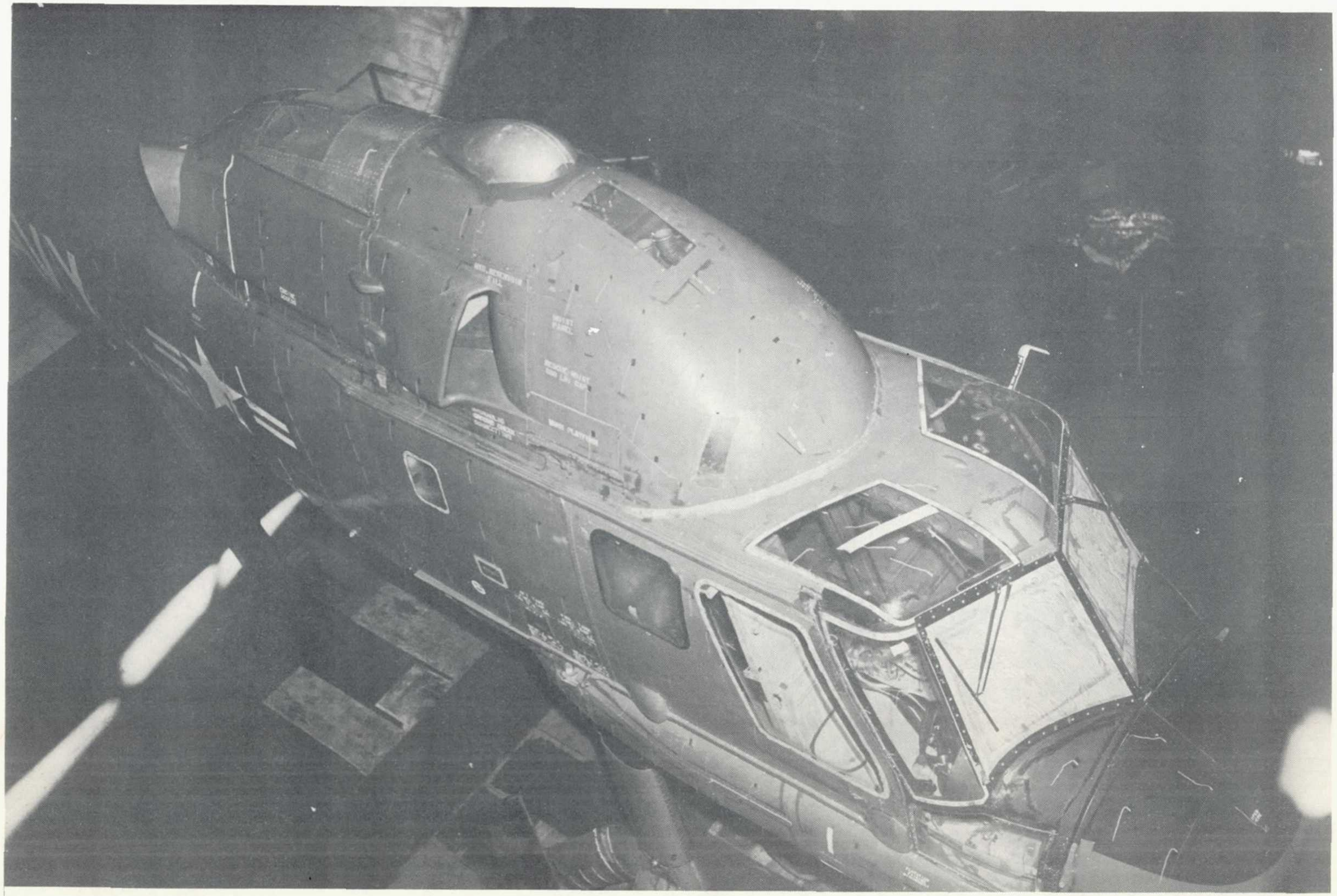

(d) View of production body showing cabin roof and engine nacelle. L-61-6065

Figure 4.- Continued.

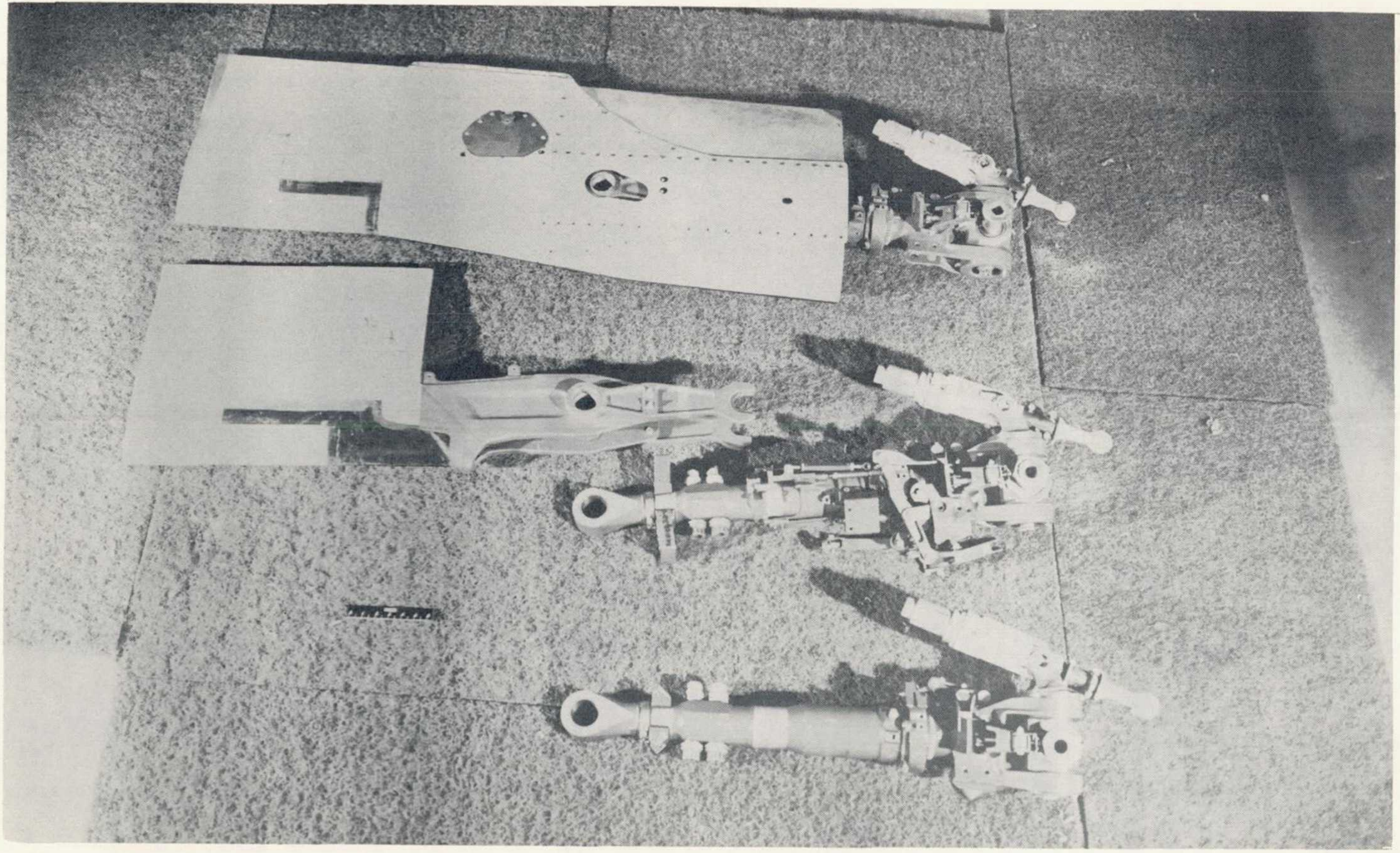

L-61-6058

(e) Blade stubs and retentions: **Top**, blade stubs and retentions with cuffs; middle, original retentions and blade stubs; lower, cleaned-up retentions.

Figure 4.- Concluded.

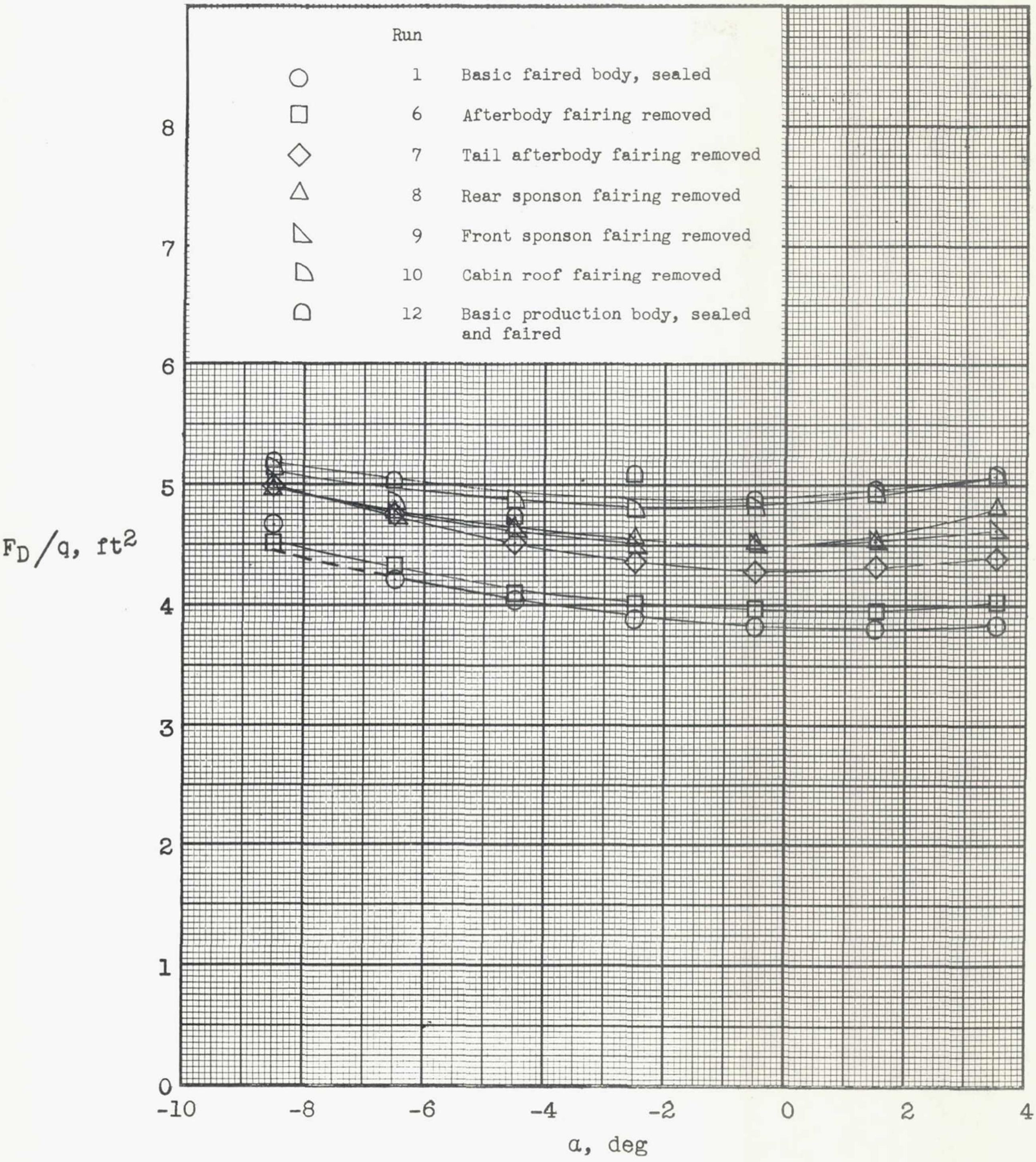

Figure 5.- Effect of body shape on the drag characteristics.

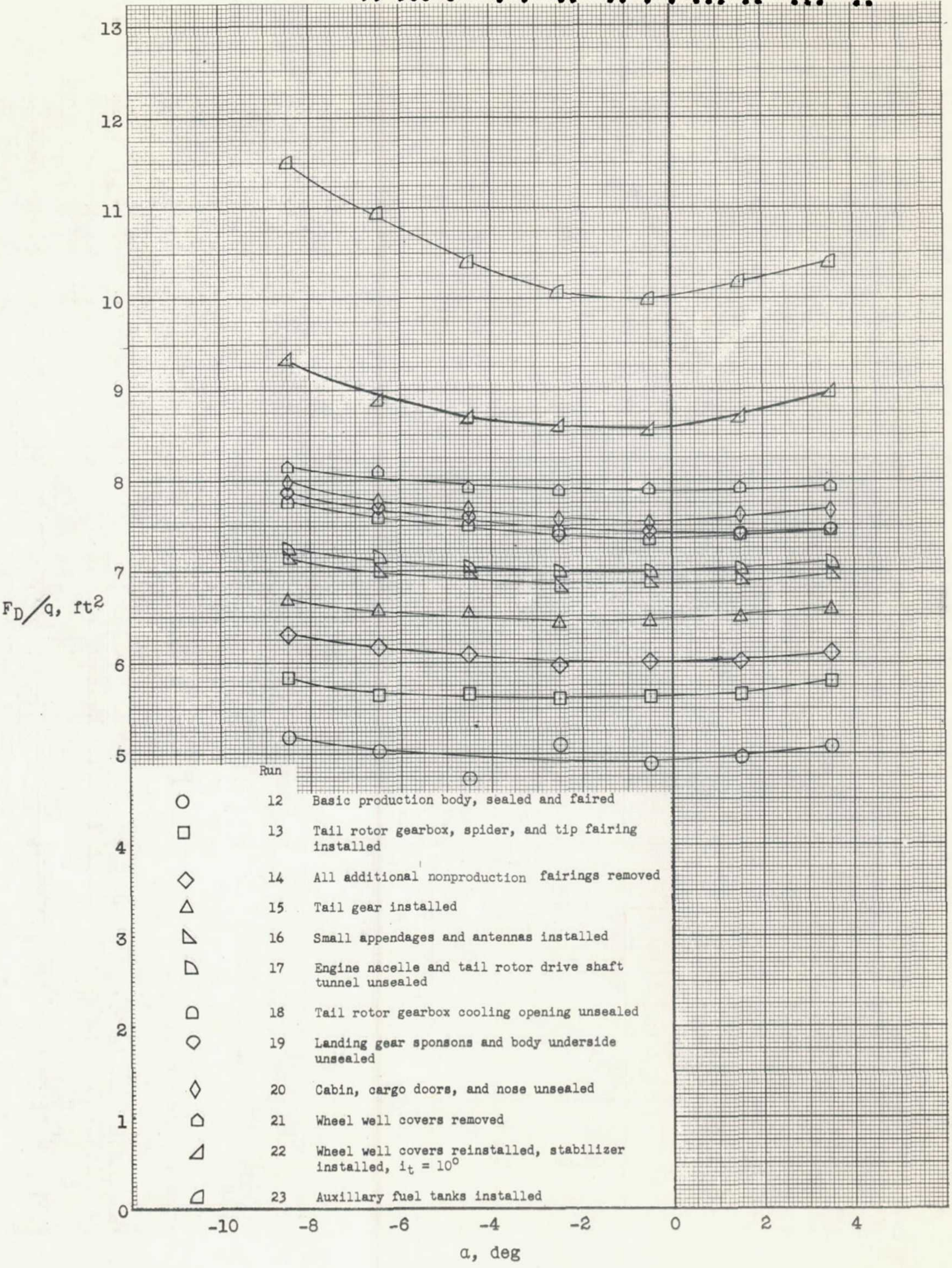

(a) Drag.

Figure 6.- Effect of appendages and leakage on the drag, lift, and pitching-moment characteristics of the fuselage.

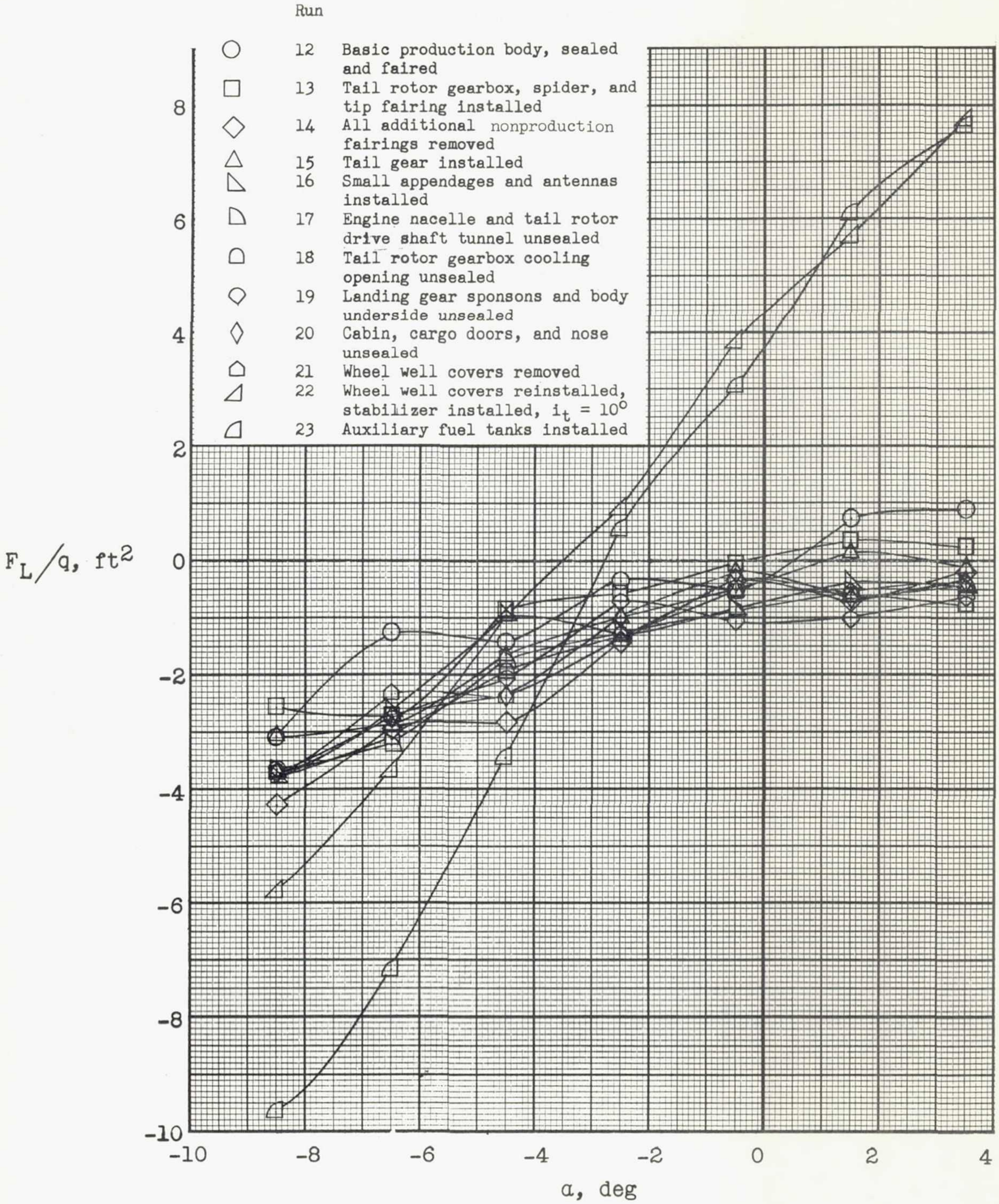

(b) Lift.

Figure 6.- Continued.

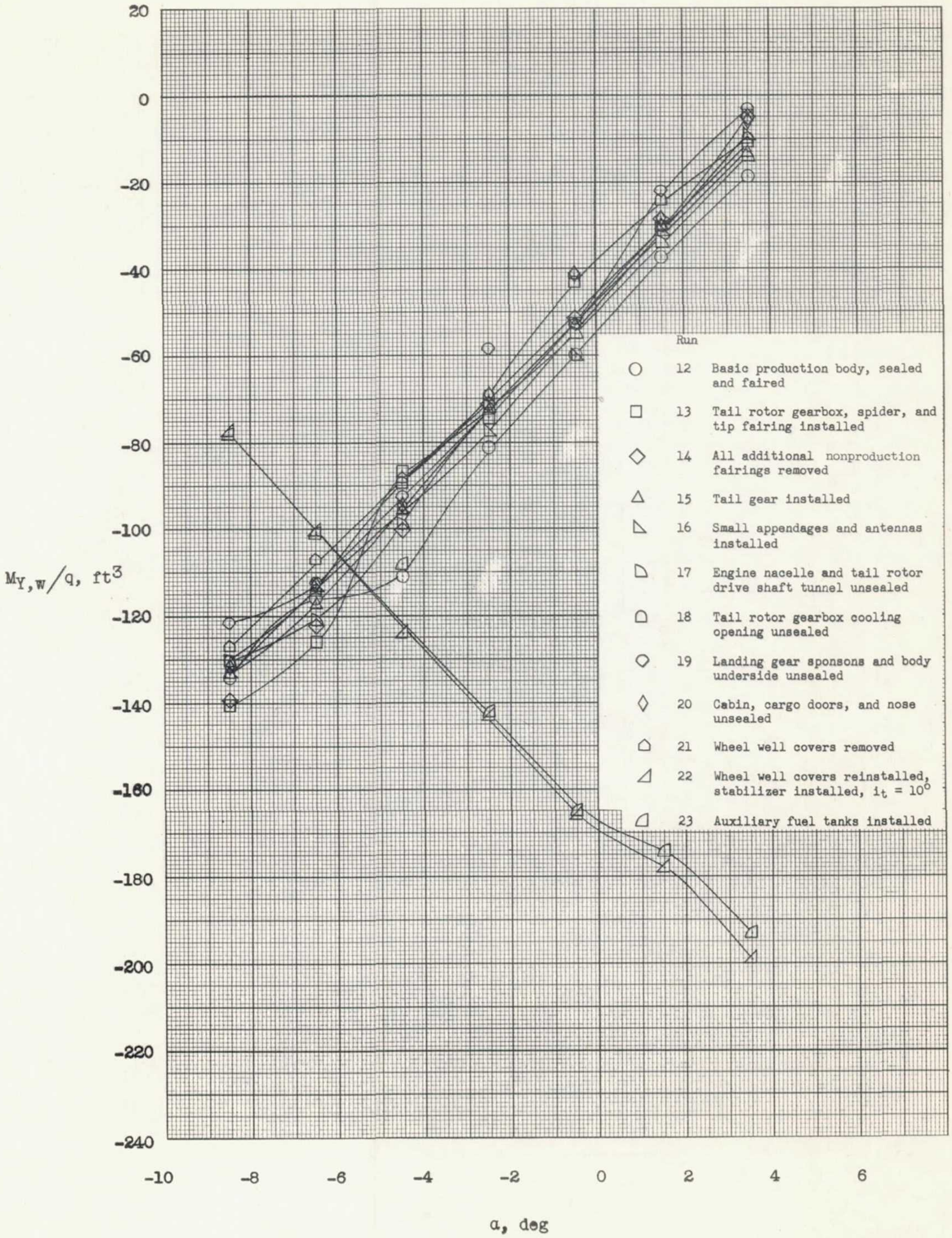

(c) Pitching moment.

Figure 6.- Concluded.

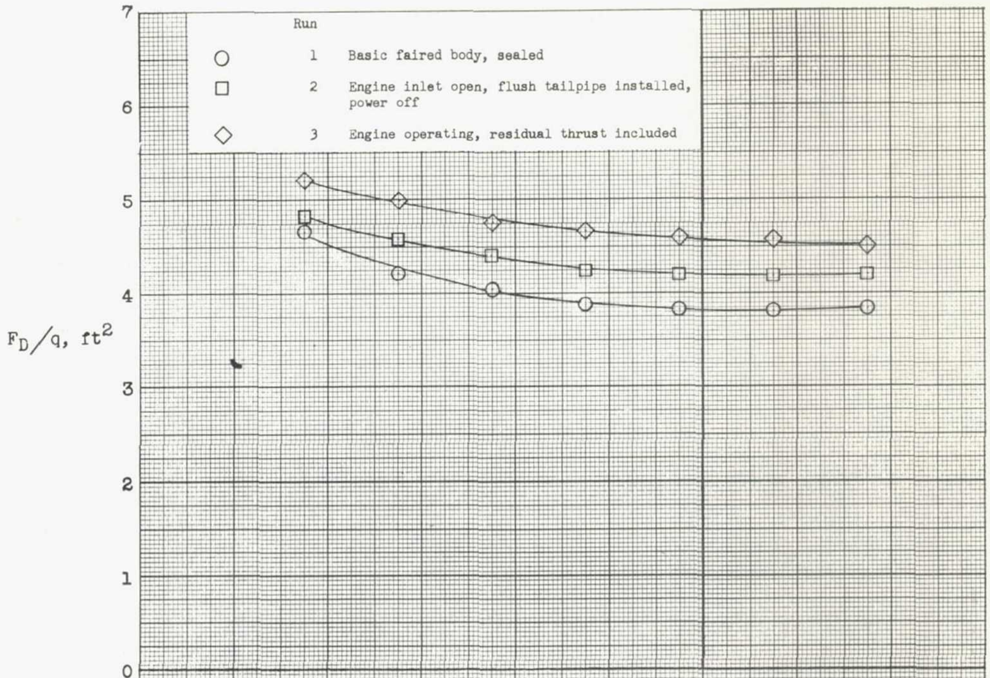

(a) Basic faired body with flush tailpipe

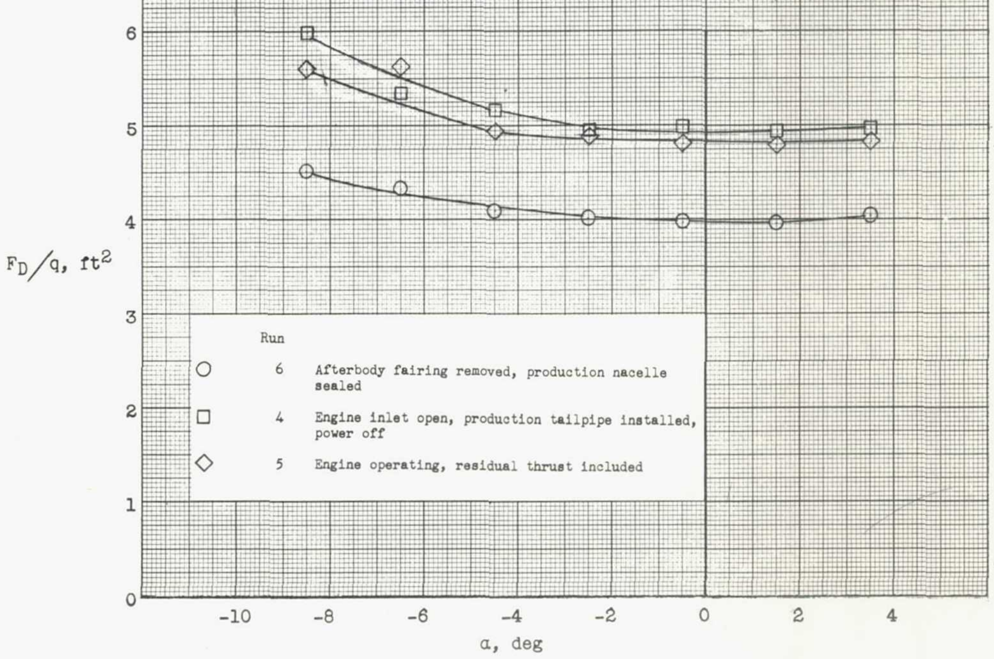

(b) Production nacelle with production tailpipe.

Figure 7.- Effect of engine operation and tailpipe configuration on the drag characteristics.

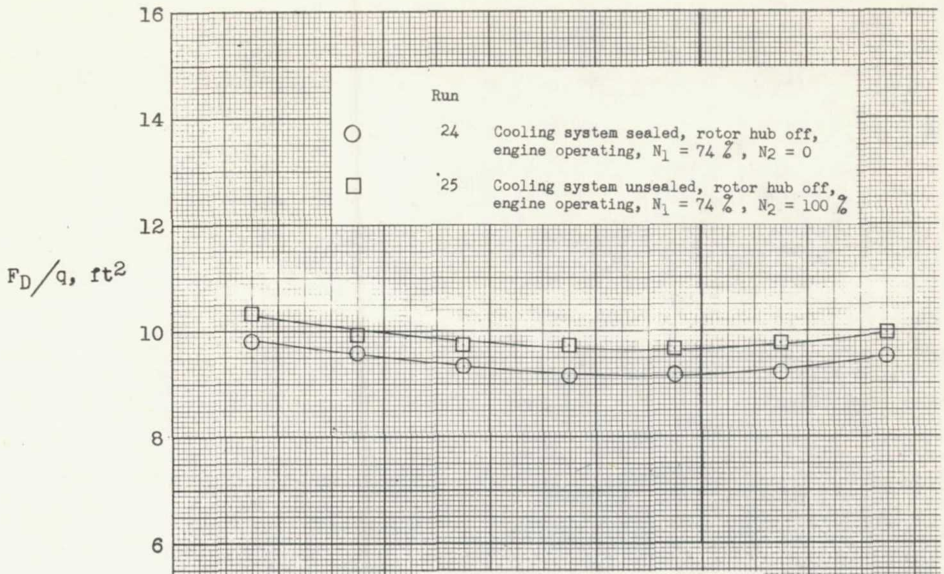

(a) Original cooling system

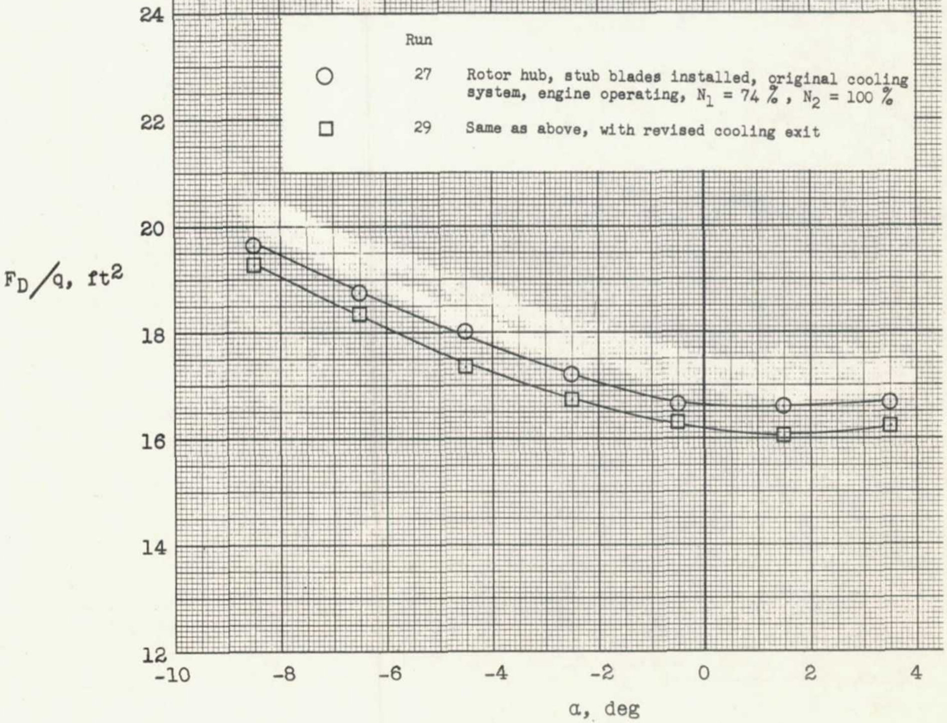

(b) Modified cooling system.

Figure 8.- Effect of cooling system on the drag characteristics. N_1, gas-generator speed; N_2, power-turbine speed.

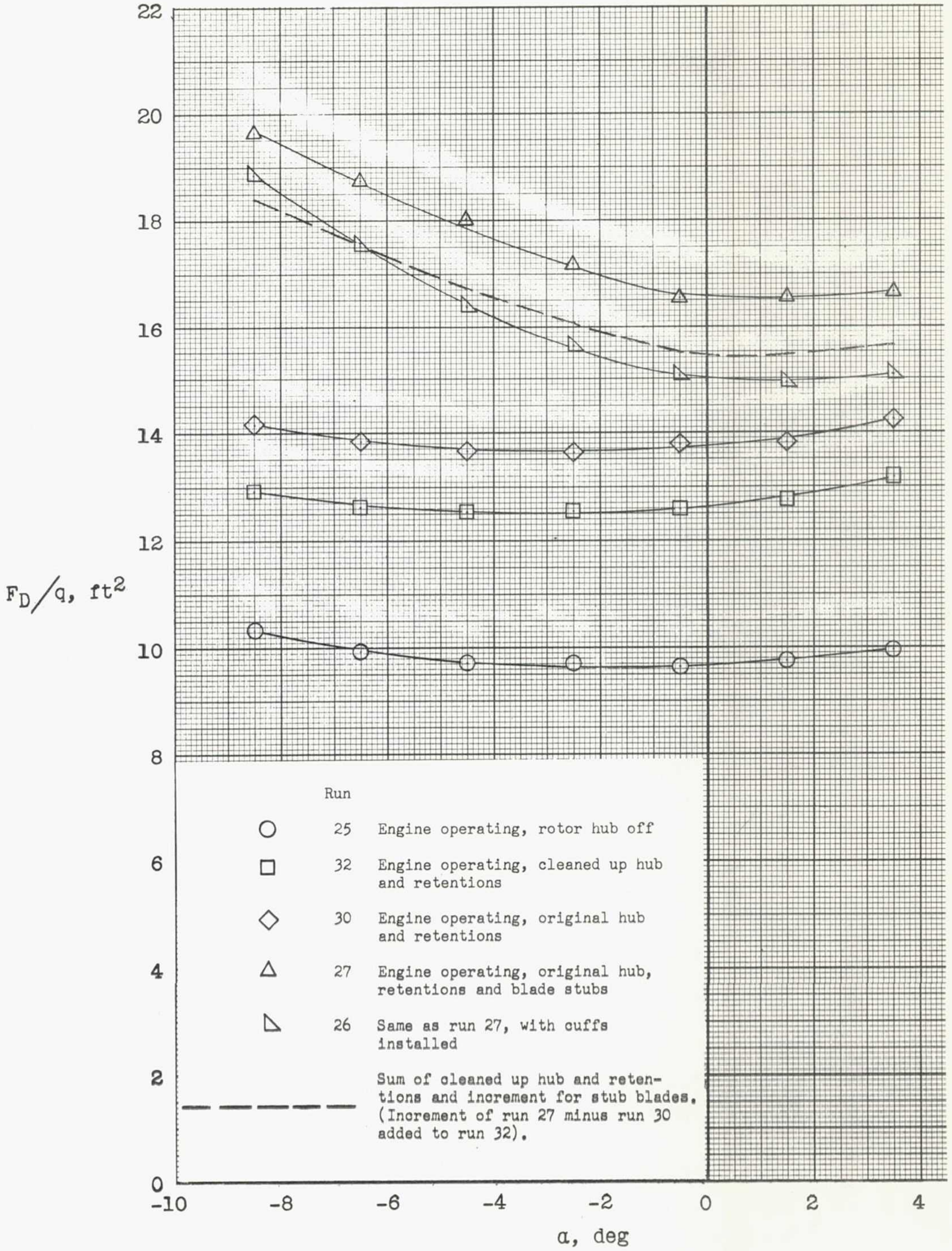

(a) Drag.

Figure 9.- Effect of rotor hub configuration on the drag, lift, and pitching-moment characteristics of the production body configuration.

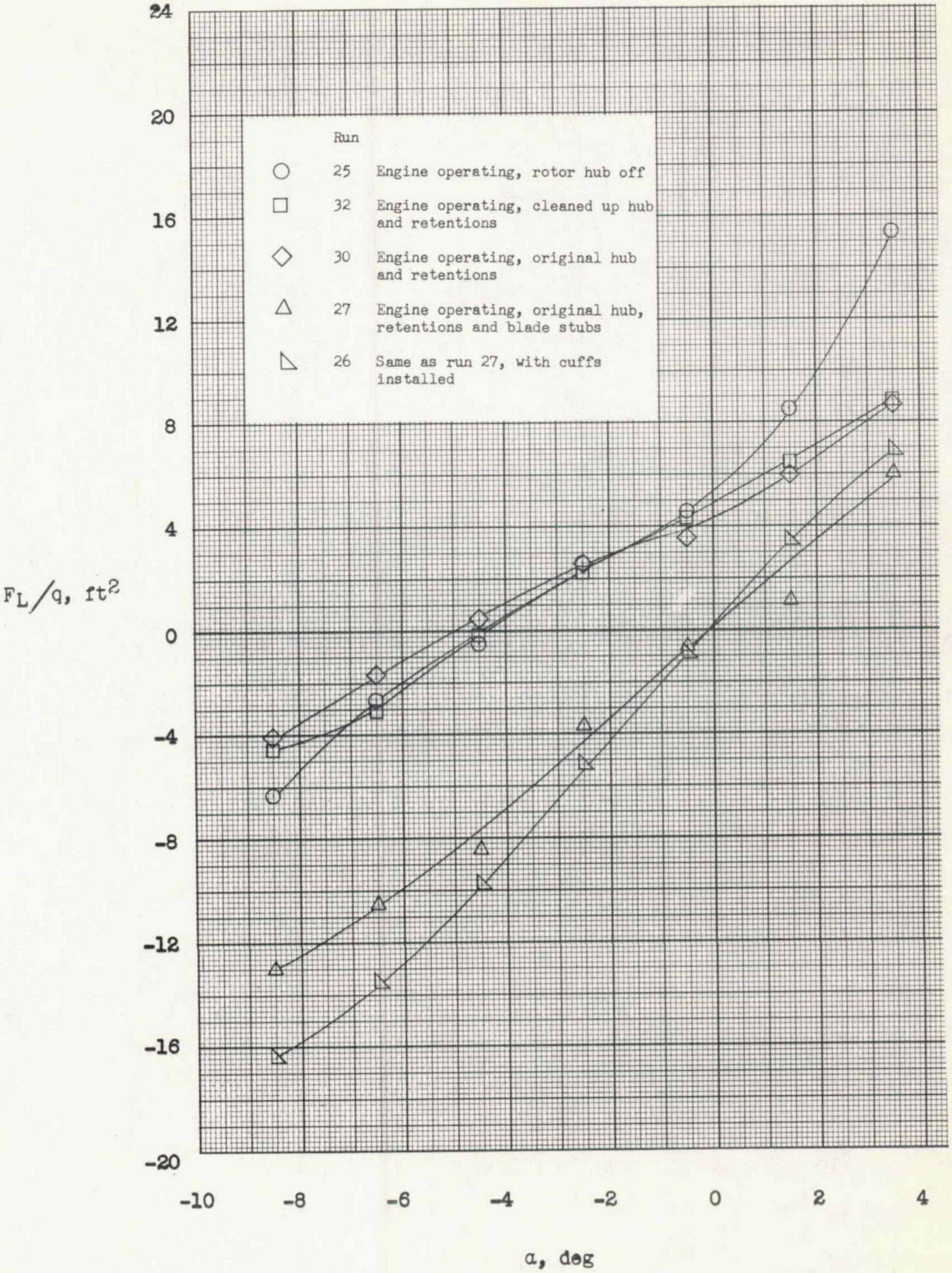

(b) Lift.

Figure 9.- Continued.

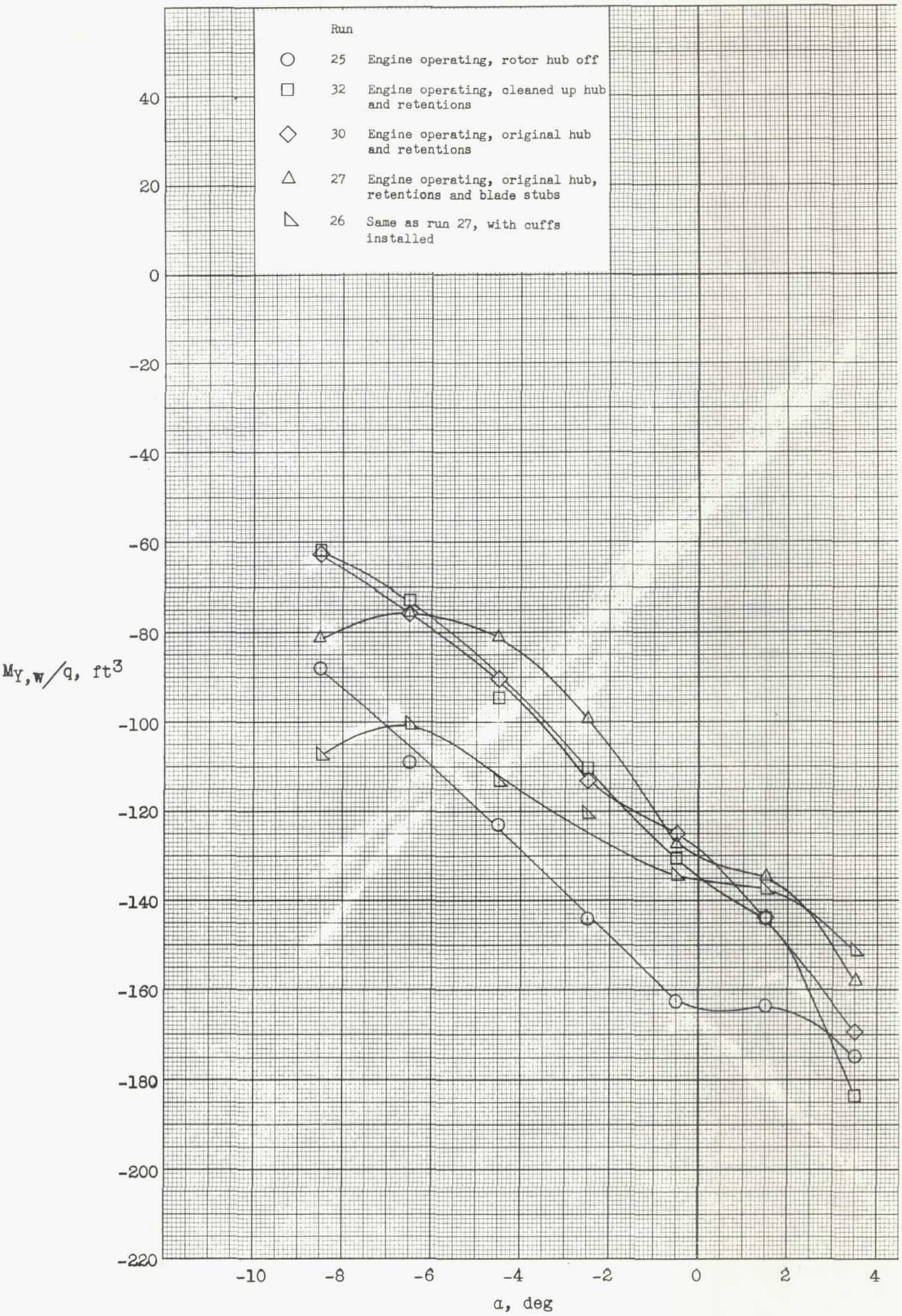

(c) Pitching moment.

Figure 9.- Concluded.

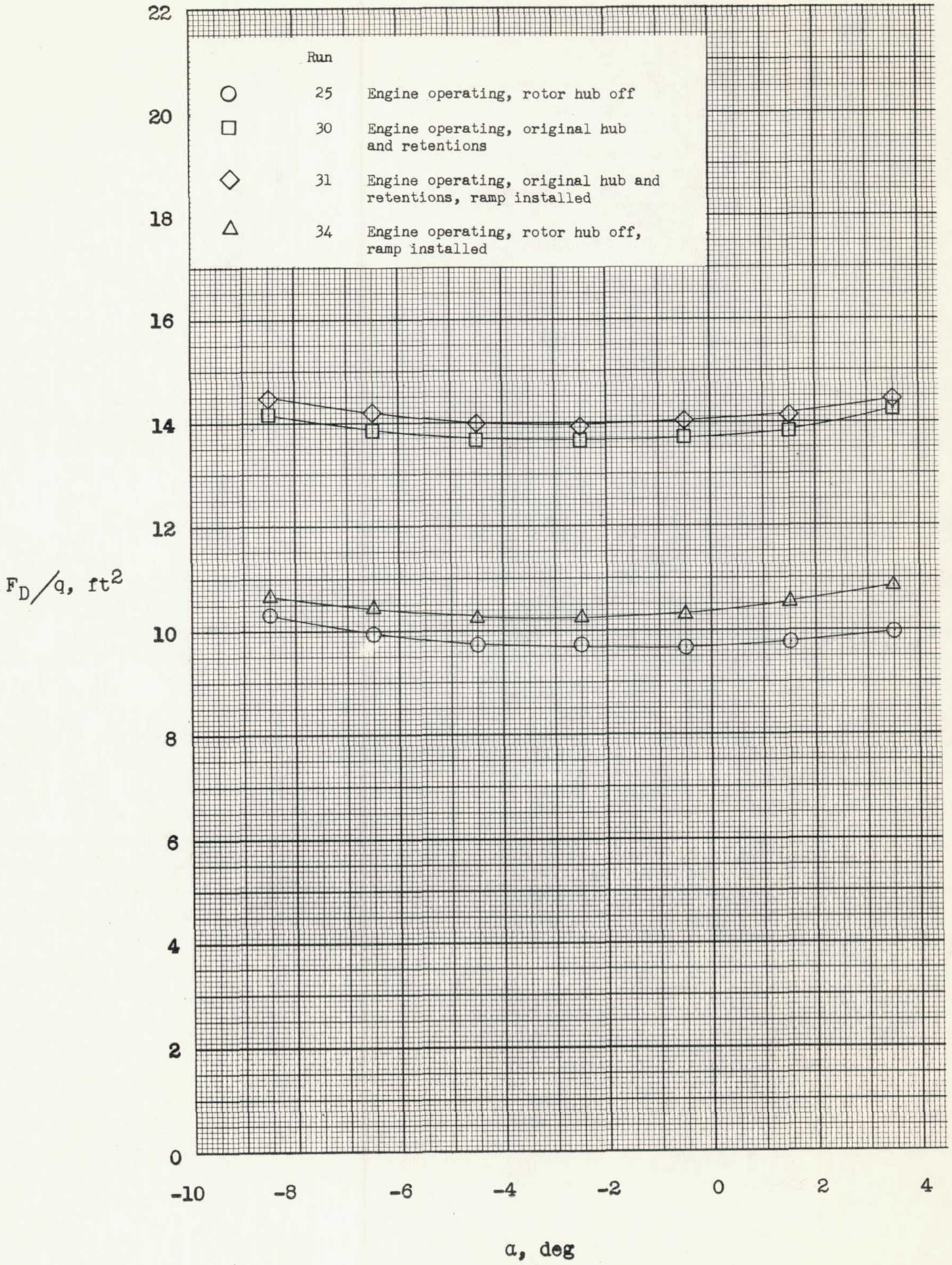

Figure 10.- Effect of ramp installed on nacelle on the drag characteristics.

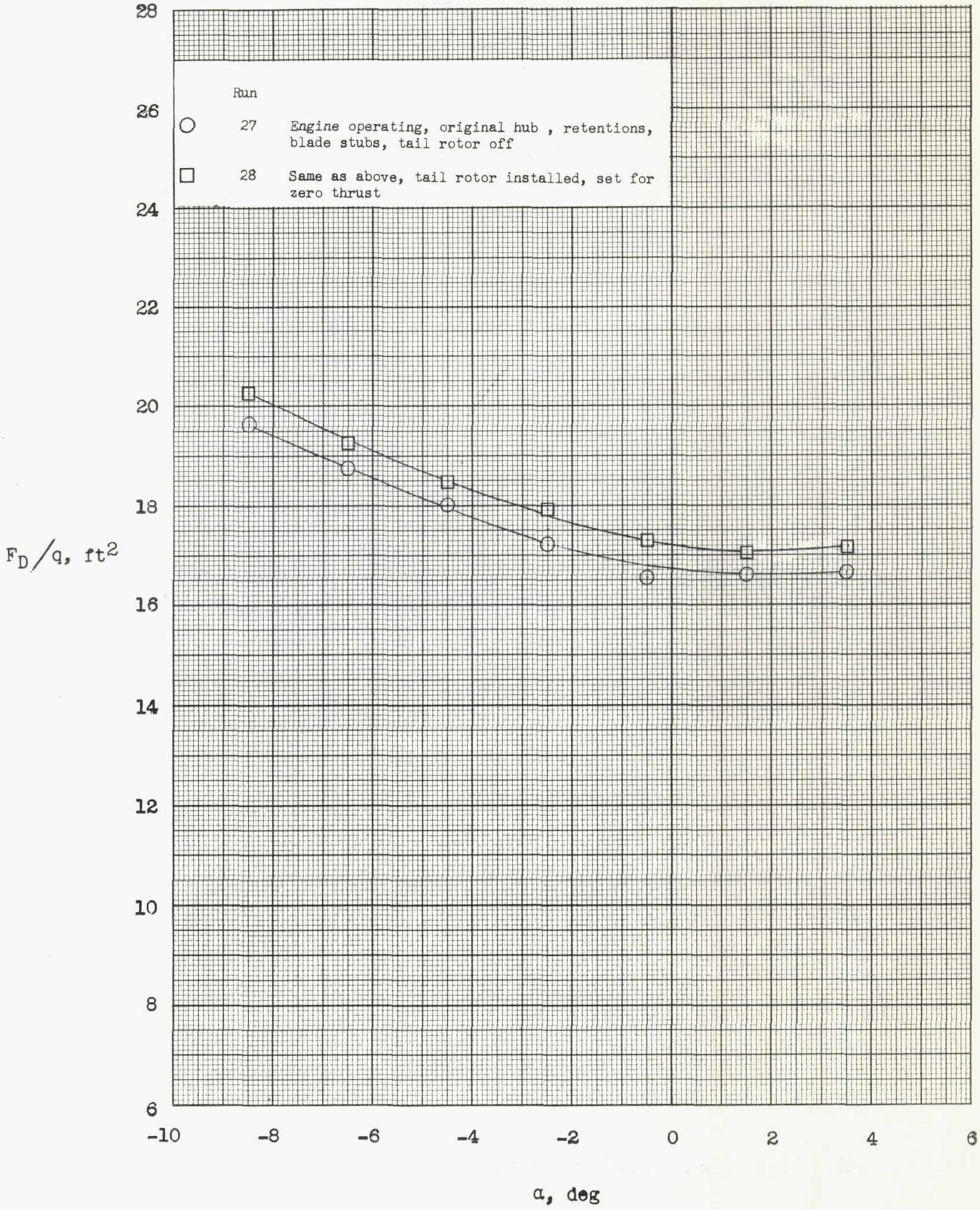

Figure 11.- Effect of tail-rotor installation on the model drag characteristics.

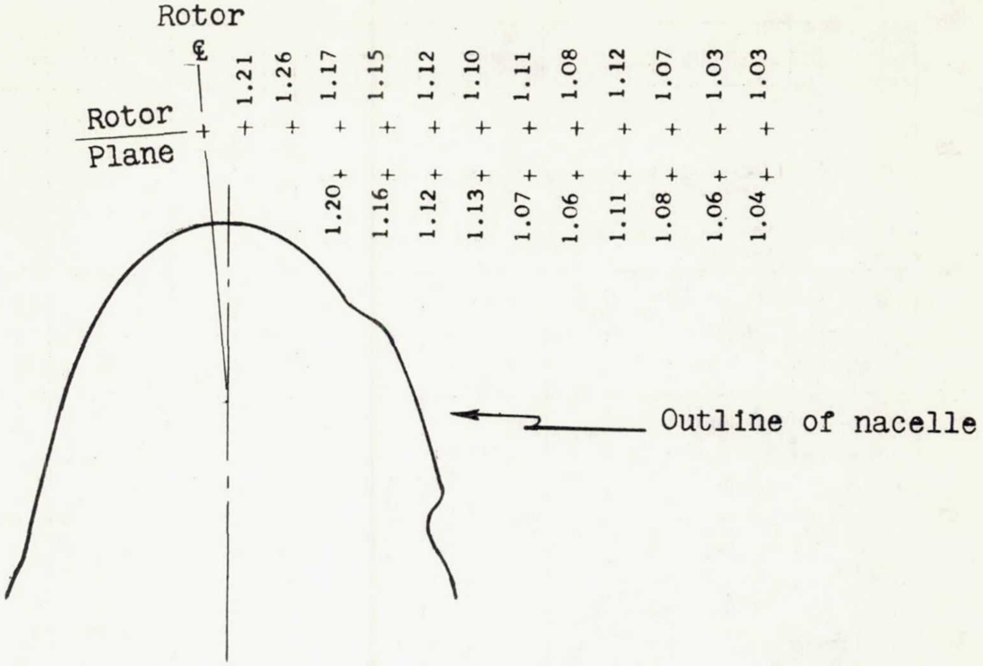

12 inches ahead of rotor shaft center line

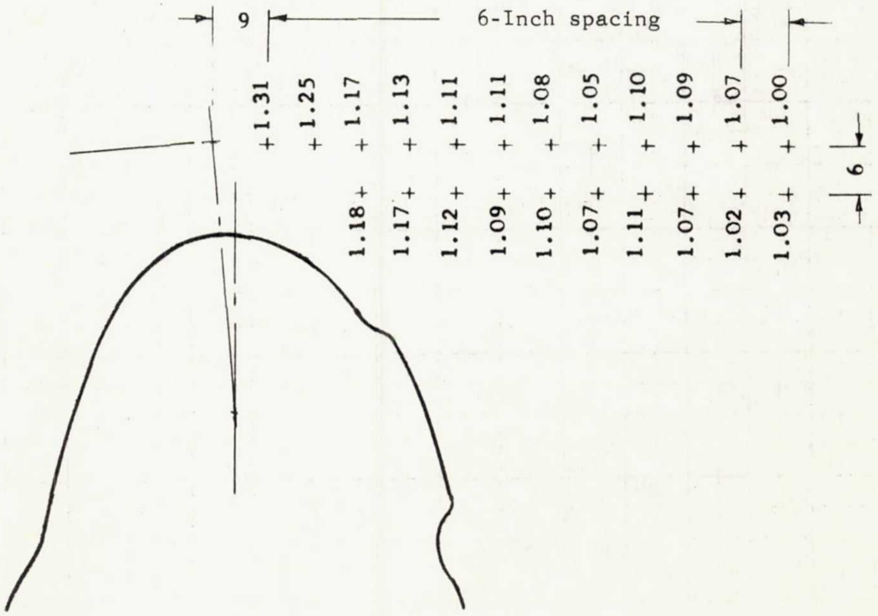

On rotor shaft center line

Figure 12.- Dynamic-pressure distribution in region of rotor hub and retentions in terms of ratio of local dynamic pressure to free-stream dynamic pressure. View from rear looking forward.

NATIONAL AERONAUTICS AND SPACE ADMINISTRATION

TECHNICAL MEMORANDUM SX-848

for the

Bureau of Weapons, Department of the Navy

FULL-SCALE WIND-TUNNEL INVESTIGATION OF THE DRAG CHARACTERISTICS OF AN HU2K HELICOPTER FUSELAGE*

TED NO. N-AM-110

By William I. Scallion

ABSTRACT

The investigation determined the effects of body shape, engine operation, appendages, and leakage on the drag of the helicopter body. The drag of the body with appendages and rotor hub, including leakage and the cooling system, was about $2\frac{3}{4}$ times that of the original sealed and faired body shape.

---

*Title, Unclassified.

DECLASSIFIED